

Investigations for Performance Improvement of X-Shaped RMSA Using Artificial Neural Network by Predicting Slot Size

Mohammad Aneesh*, Ashish Singh, Jamshed A. Ansari, Kamakshi, and Saiyed S. Sayeed

Abstract—In this paper, an application of artificial neural network based on multilayer perceptron (MLP) model is presented for predicting the slot size on the radiating patch for improvement of the performance of patch antenna. Several performance affecting parameters like resonance frequencies, gain, directivity, antenna efficiency, and radiation efficiency for dual band frequency are observed with the variation of slot size. For validation of this work, a prototype X-shaped patch antenna is fabricated using glass epoxy substrate and its performance parameters are measured experimentally and have been found in good agreement with ANN and simulated values.

1. INTRODUCTION

Microstrip antennas (MSAs) are very popular among the researchers due to their attractive features, such as low profile, light weight, compatibility with monolithic microwave integrated circuits, low fabrication cost, and single, dual, multiband frequency operations etc. [1]. Due to these features of MSA for dual and multiband operation, it has attracted most of the researchers since single antenna can be used for more than two applications. To explore dualband MSA many techniques have been suggested by researchers for achieving dual frequency band [2–4], these are by inserting slots and notches, stacking of substrate etc.. All these available techniques are based on the numerical and analytical methods. Analytical methods are easy and specified to only definite shapes of the patch. These methods are not suitable for thick substrate. Whereas, numerical methods are suitable for all shapes of the MSA and require much more time in solving mathematical equations. For every minor change in geometry, it needs new solution, so it becomes time consuming and lengthy process. For reducing some of these problems, an ANN model is proposed for predicting the slot size over a desired level of performance parameters for achieving dualband frequency operation.

Over the last decade artificial neural network (ANN) adopts remarkable importance in field of wireless communication due to its fast and accurate modelling, simulation, and optimization. In ANN model, the measured, simulated, and calculated data are used for training. Trained ANN model predicts accurate slot size for every small variation in the geometry both for thin and thick substrates. The purpose behind the training of ANN model is to minimize the error between actual output and reference output. The use of ANN in rectangular microstrip patch antenna (RMSA) has been proposed in [5–8]. Further, Watson et al. [9] developed an ANN model for microwave components. Different ANN models [10–18] were used for analyzing and synthesizing of microstrip patch antennas. Few other neural models have been proposed for slot loaded microstrip patch antennas in [19, 20]. Robustillo et al. [21] have designed a contoured-beam reflectarray for a EuTELSAT European coverage using stacked patch element with the help of ANN. Thereafter, an ANN based synthesis has been suggested in [22, 23] for a single feed circularly-polarized truncated corners square MSA and for reflectarray antennas respectively. Further, an application of ANN for computing resonant frequency of E-shaped compact patch antenna has been proposed in [24]. An ANN based synthesis model has been proposed for predicting the

Received 28 December 2013, Accepted 26 January 2014, Scheduled 30 January 2014

* Corresponding author: Mohammad Aneesh (aneeshau14@gmail.com).

The authors are with the Department of Electronics & Communication, University of Allahabad, Allahabad, U.P., India.

size of slot on the radiating patch and inserting gap between ground plane and substrate sheet by Khan et al. [25]. It is very much essential for the antenna designers to predict the slot-size for desired level of performance parameters. In this paper, an artificial neural model is presented for the prediction of accurate slot size to achieve desired level of accuracy for antenna parameters such as $2 \text{ GHz} \leq \text{resonance frequency} \leq 8 \text{ GHz}$, $2 \text{ dBi} \leq \text{gain} \leq 9 \text{ dBi}$, $5 \text{ dBi} \leq \text{directivity} \leq 9.8 \text{ dBi}$, $70\% \leq \text{antenna efficiency} \leq 100\%$, and $75\% \leq \text{radiation efficiency} \leq 100\%$ for dualband frequency.

In this paper, an ANN model is proposed for achieving desired level of performance with inserting X-shape slot on the radiating patch. The fabricated X-shaped RMSA is investigated for dual band frequency operation so that the single antenna can be utilized for more than one frequency operation; whereas, accurate slot size is predicted by ANN model for a desired level of performance.

2. DESIGN OF PROPOSED ANTENNA AND SAMPLE GENERATION

The proposed antenna geometry of the microstrip patch antenna is shown in Figure 1. Here a rectangular patch of dimensions $L = 23 \text{ mm}$, $W = 23 \text{ mm}$ is used with a ground plane of dimension $L_g = 55 \text{ mm}$, $W_g = 55 \text{ mm}$. The antenna is simulated by method of moments (MoM) based on IE3D simulation software using glass epoxy substrate whose dielectric constant (ϵ_r) is 4.4, height (h) is 1.60 mm and loss tangent $\tan \delta = 0.002$ for dualband frequency operation. SMA connector is used for the excitation of proposed patch antenna. Specified range of slot size is shown in Table 1 for the generation of samples of patch antenna used for training and testing of the ANN model. These samples are generated in IE3D software [26].

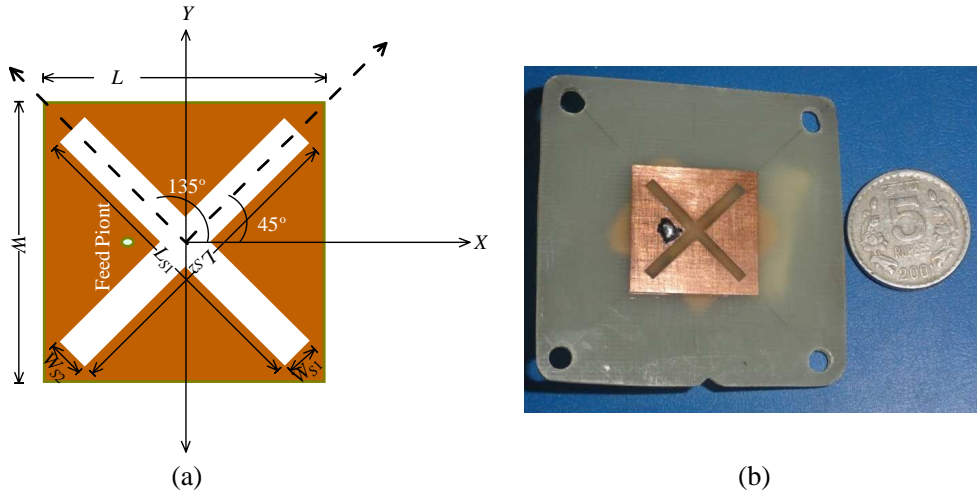


Figure 1. (a) X-shaped RMSA. (b) Fabricated X-shaped RMSA.

Table 1. Sampling of slot size.

Slot size	Specified range	Step size	Generated samples
L_{s1}	$1 \text{ mm} \leq L_{s1} \leq 25 \text{ mm}$	$50 \mu\text{m}$	500 samples
W_{s1}	$0.5 \text{ mm} \leq W_{s1} \leq 5 \text{ mm}$	$10 \mu\text{m}$	(for training 400 samples)
L_{s2}	$1 \text{ mm} \leq L_{s2} \leq 25 \text{ mm}$	$50 \mu\text{m}$	(for testing 100 samples)
W_{s2}	$0.5 \text{ mm} \leq W_{s2} \leq 5 \text{ mm}$	$10 \mu\text{m}$	

3. NEURAL NETWORK MODELLING

Multilayer perceptron (MLP) neural network consists of input layer, output layer, and single or more than one hidden layers. The role of each layer in ANN model is different. The MLP neural network

uses three basic common steps for the training purpose. Firstly training samples are generated, then in second step, structure of the hidden layer is selected, and finally in third step weights and biases are adjusted using algorithm. For the testing of ANN model, a sample set of data is used which are not included in training samples. ANN toolbox of MATLAB software [27] is used here for training and testing of the ANN model.

Four variable output of the proposed ANN model is computed as [28]

$$O_i = f_3 ([W_O] (f_2 ([W_S] (f_1 ([W_F][P_i] + [B_F])) + [B_S])) + [B_O]) \quad (1)$$

where four variable output

$$[O_i] = \begin{bmatrix} L_{S1} \\ W_{S1} \\ L_{S2} \\ W_{S2} \end{bmatrix} \quad (2)$$

where $[P_i]$ is 10 variable input parameters

$$[P_i] = [f_1 \quad f_2 \quad d_1 \quad d_2 \quad g_1 \quad g_2 \quad E_{a1} \quad E_{a2} \quad E_{r1} \quad E_{r2}] \quad (3)$$

Weight matrix of the first hidden layer

$$[W_F] = \begin{bmatrix} W_{F1,1} & W_{F1,2} & \dots & W_{F1,10} \\ W_{F2,1} & W_{F2,2} & \dots & W_{F2,10} \\ \cdot & \cdot & \dots & \cdot \\ \cdot & \cdot & \dots & \cdot \\ W_{F50,1} & W_{F50,2} & \dots & W_{F50,10} \end{bmatrix} \quad (4)$$

Weight matrix of the second hidden layer

$$[W_S] = \begin{bmatrix} W_{S1,1} & W_{S1,2} & \dots & W_{S1,50} \\ W_{S2,1} & W_{S2,2} & \dots & W_{S2,50} \\ \cdot & \cdot & \dots & \cdot \\ \cdot & \cdot & \dots & \cdot \\ W_{S50,1} & W_{S50,2} & \dots & W_{S50,50} \end{bmatrix} \quad (5)$$

Bias matrix of the first layer

$$[B_F] = \begin{bmatrix} b_{f1} \\ b_{f2} \\ \cdot \\ \cdot \\ b_{f10} \end{bmatrix} \quad (6)$$

Bias matrix of the second layer

$$[B_S] = \begin{bmatrix} b_{S1} \\ b_{S2} \\ \cdot \\ \cdot \\ b_{S50} \end{bmatrix} \quad (7)$$

Biases of the output layer

$$[B_O] = \begin{bmatrix} b_{O1} \\ b_{O2} \\ b_{O3} \\ b_{O4} \end{bmatrix} \quad (8)$$

The mean square errors (MSE) will be computed as [10],

$$MSE = \frac{1}{n} \sum_{i=1}^n [O_i - F_{ANN}(P_i)]^2 \quad (9)$$

3.1. Training and Testing Sample Generation

In this section, sample generation for training and testing of proposed geometry is performed with varying the first slot length, width (L_{s1} , W_{s1}) and second slot length, width (L_{s2} , W_{s2}) whereas inclination angles of slots $\alpha_1 = 45^\circ$ and $\alpha_2 = 135^\circ$ with x -axis of the patch. In this section, a total number of 400 samples are generated for the training, and 100 samples are generated for testing of proposed antenna geometry on varying the slots length and width (L_{s1} , W_{s1} , L_{s2} , W_{s2}). Different other performance parameters for proposed geometry at dual resonance frequencies (f_1 , f_2), directivities (d_1 , d_2), gains (g_1 , g_2), antenna efficiencies (E_{a1} , E_{a2}), and radiation efficiencies (E_{r1} , E_{r2}) are observed with the variation of slots length and width (L_{s1} , W_{s1} , L_{s2} , W_{s2}) whereas inclination angle of slots with the x -axis $\alpha_1 = 45^\circ$ and $\alpha_2 = 135^\circ$ is kept constant. Hence a matrix of performance parameters $[P_i] = [f_1 f_2 d_1 d_2 g_1 g_2 E_{a1} E_{a2} E_{r1} E_{r2}]$ is achieved with the variation of slots length and width which is in matrix of $[O_i] = [L_{s1} W_{s1} L_{s2} W_{s2}]$. Here a reverse synthesis is used for ANN modeling.

3.2. Proposed Structure of ANN Model and Training

For the present work a four layer multilayer perceptron feed forward back propagation (MLPFFBP) ANN is used with 7 different training algorithms for training of the data set of proposed antenna geometry. For the best performance configuration of ANN model is selected 10-50-50-4, means 10 neurons in input layer, 50-50 neurons in the first and second hidden layer and 4 neurons in output layer with learning rate (η) = 0.1, momentum coefficient (μ) = 0.75, error goal (e_g) = 0.001, and MSE = 1.31×10^{-6} . MLP model is trained with seven different algorithms BFGS quasi-Newton (BFG), Bayesian regulation (BR), scaled conjugate gradient (SCG), Powell-Beale conjugate gradient (CGB), conjugate gradient with Fletcher-Peeves (CGF), one step secant (OSS), and Levenberg-Marquardt (LM), respectively [29]. Among these training algorithms LM gives best accuracy for MLP model training, whereas, the weight and biases of the first and second hidden layer is automatically adjusted between 0 and 1. For the testing of remaining 100 samples of antenna parameters are used in ANN model, which predict the accurate size of slots length and width (L_{s1} , W_{s1} , L_{s2} , W_{s2}) for a given set of resonant frequencies, gains, directivities, antenna efficiencies, and radiation efficiencies for dual band resonance.

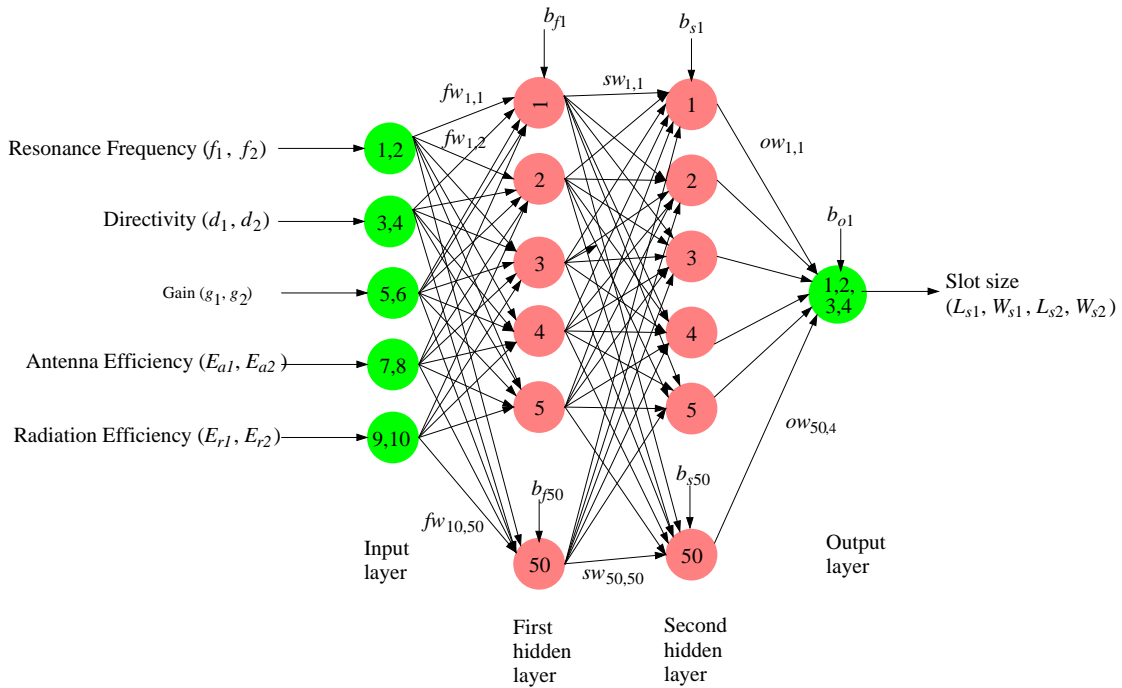


Figure 2. Artificial neural network (ANN) model.

4. EXPERIMENTAL RESULTS AND DISCUSSION

The structure of MLPFFBP-ANN is shown in Figure 2, training and testing of ANN model using different algorithm is discussed in previous section. Here it is observed that the LM training algorithm is most superior than the other training algorithms BFG, BR, SCG, CGB, CGF, OSS which requires less computational time with minimum errors for the prediction of slot size as shown in Figures 3 and 4.

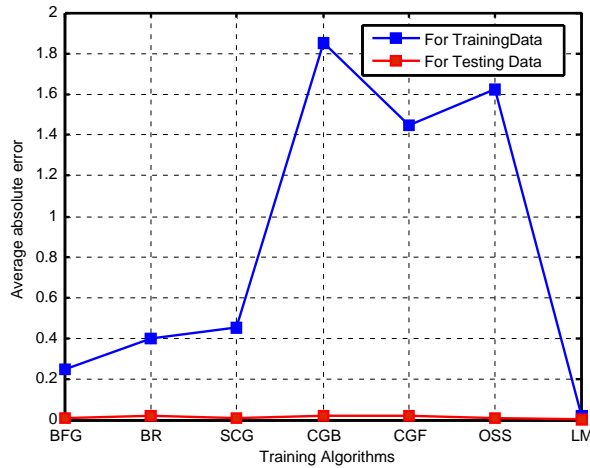


Figure 3. Comparison of training algorithms with average absolute errors for MLPFFBP-ANN.

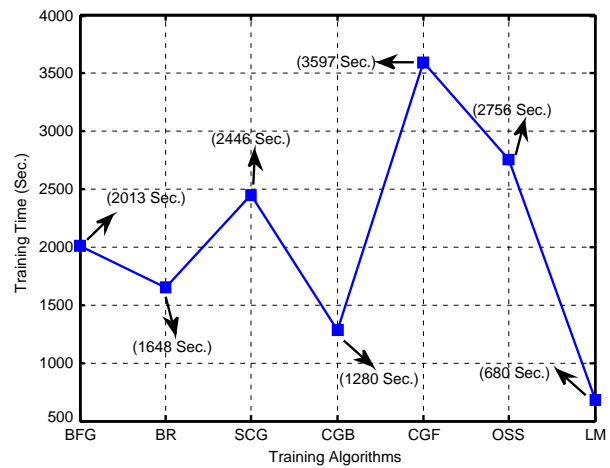


Figure 4. Comparison of training algorithms with training time for MLPFFBP-ANN.

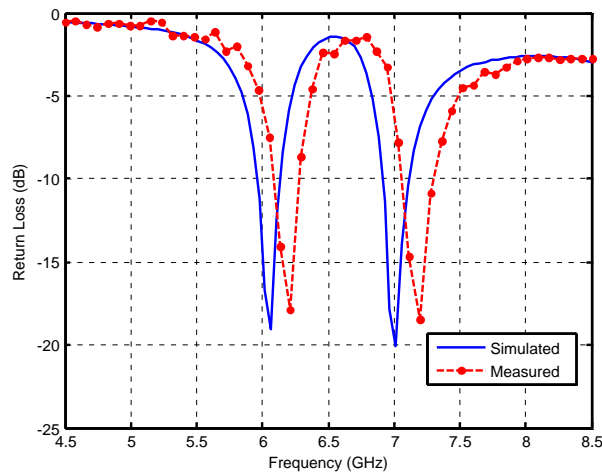


Figure 5. Variation of simulated and measured return loss with frequency.

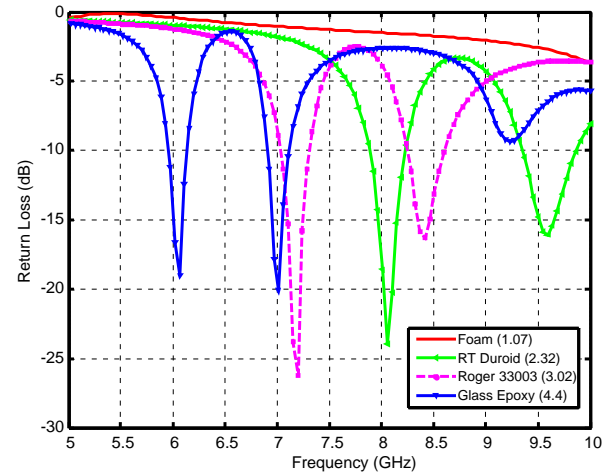


Figure 6. Variation of return loss with several dielectric substrates.

Table 2. Slot size (Simulated and ANN output value).

Parameter	IE3D Simulated Value	ANN Output Value
L_{s1}	22 mm	22.014 mm
W_{s1}	2 mm	2.010 mm
L_{s2}	22 mm	22.016 mm
W_{s2}	2 mm	2.011 mm

4.1. Results of Validation Study

For the validation of this work, an X-shaped RMSA is fabricated using glass epoxy substrate as shown in Figure 1(b). The patch dimension ($L \times W$) is $23 \times 23 \text{ mm}^2$, etched on the upper side of the substrate. In this patch two slots are etched of 22 mm length (L_{s1}, L_{s2}) and 2 mm width (W_{s1}, W_{s2}) with inclination angle $\alpha_1 = 45^\circ$ and $\alpha_2 = 135^\circ$ from the x -axis of patch. This X-shaped MSA is excited by a probe feed, which helps the electromagnetic waves to propagate in the direction of normal to the patch. A SMA connector is used for RF connection which operating frequency range is 0–18 GHz. The return loss of fabricated antenna is measured using Agilent N5230A network analyzer and the radiation pattern measurement of the X-shaped RMSA is done in anechoic chamber with precautions. Simulated and ANN output values of slot size for X-shaped RMSA is given in Table 2.

Figure 5 shows the comparison between simulated and measured values of return loss ($S_{11} \leq -10 \text{ dB}$) for X-shaped RMSA. It is observed that this antenna operates at dual frequency bands at 6 GHz, and 7 GHz, which is useful for wireless satellite communication applications. Simulated and experimental results are in close agreement, only small variation is occurred and it may be probably due to irregularity in fabricating the X-shaped RMSA, the size and losses of the solder joints which is not considered in simulation.

Figure 6 shows the variation of dielectric constant at fixed height of the substrate. It is observed

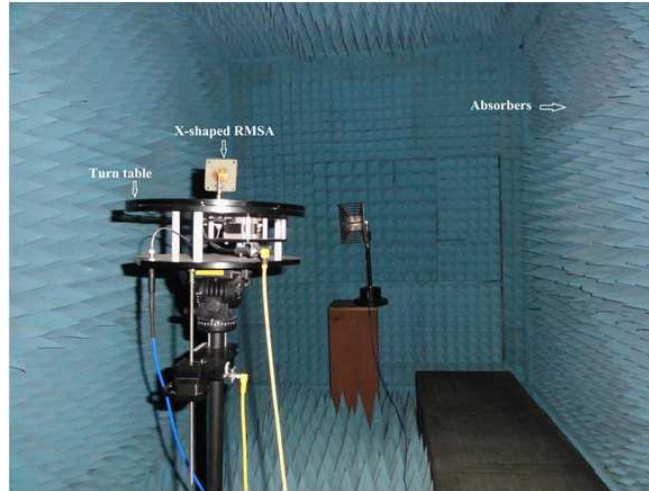


Figure 7. Anechoic chamber experimental setup for radiation pattern measurement of X-shaped RMSA.

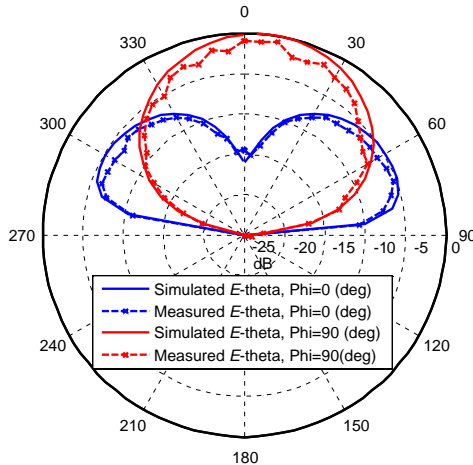


Figure 8. Radiation pattern of X-shaped RMSA at 6 GHz.

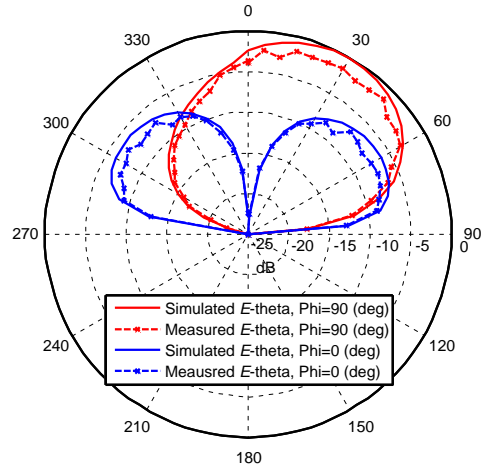


Figure 9. Radiation pattern of X-shaped RMSA at 7 GHz.

that on reducing the dielectric constant from glass epoxy to foam, lower and upper resonance frequencies shift towards higher side. This is because resonance is inversely proportional to square root of dielectric constant.

The radiation pattern of X-shaped RMSA is measured in anechoic chamber. Experimental setup is shown in Figure 7. The simulated and measured radiation pattern of the proposed antenna is shown in Figures 8–9. It is observed that simulated and measured results obtained are in close agreement at lower and upper resonance frequencies of 6 GHz and 7 GHz respectively. The radiation pattern of the proposed antenna is measured in anechoic chamber and the distance between the transmitting and receiving antenna is 200 cm. It is also investigated that 3 dB beam width of antenna at frequency 6 GHz is 50° (measured) and 51.0001° (simulated) for E -theta, $\phi = 0^\circ$ whereas for E -theta, $\phi = 90^\circ$, it is 72° (measured) and 73.2885° simulated). The tilt angle of the direction of maximum radiation is 31° and the 3 dB beam width about 51° (simulated) and 50° (measured) at upper resonant frequency of 7 GHz for E -theta, $\phi = 0^\circ$ whereas for E -theta, $\phi = 90^\circ$ it is found 66.88° (simulated) and 64° (measured). In anechoic chamber E -theta, $\phi = 0^\circ$ is measured in x - z plane whereas E -theta, $\phi = 90^\circ$

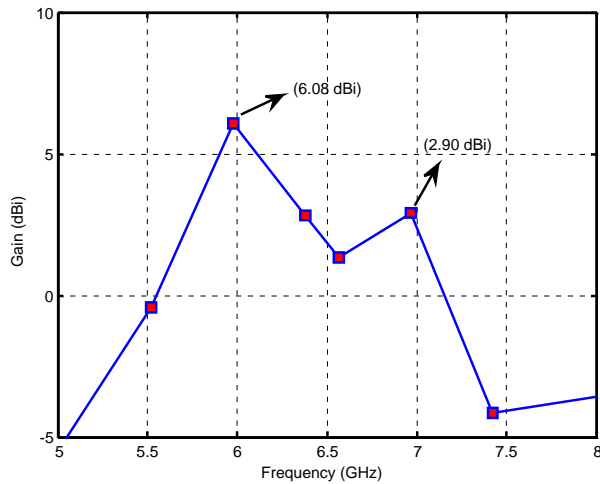


Figure 10. Comparison between gain vs frequency of X-shaped RMSA.

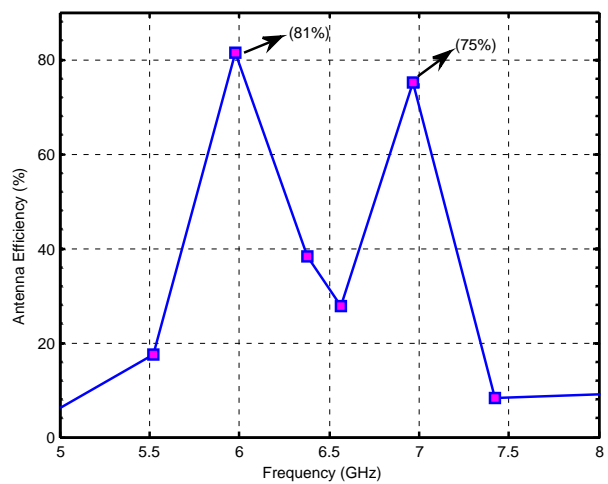


Figure 11. Comparison between antenna efficiency (%) vs frequency of X-shaped RMSA.

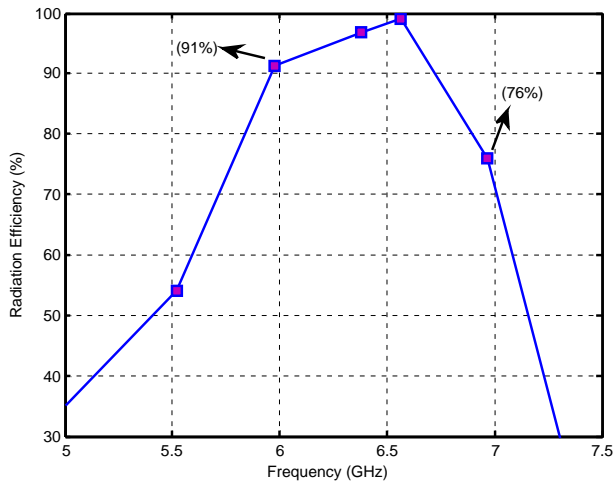


Figure 12. Comparison between radiation efficiency (%) vs frequency of X-shaped RMSA.

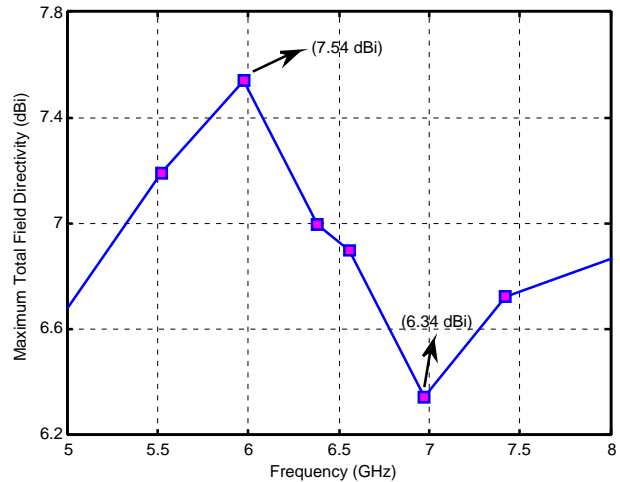


Figure 13. Comparison of maximum total field directivity vs frequency of X-shaped RMSA.

in measured in x - y plane.

The peak gain of the patch antenna at operating frequencies of 6 GHz and 7 GHz is shown in Figure 10. It is observed that at resonating frequencies of 6 GHz and 7 GHz, peak gain is 6.08 dBi and 2.90 dBi respectively. Figure 11 shows the antenna efficiency over the operating dual frequency. It is observed that antenna efficiency is 81% at 6 GHz and 75% at 7 GHz. Figure 12 shows the radiation efficiency over the operating frequency and it is found that its values are 91% at 6 GHz and 76% at 7 GHz. The variation of maximum total field directivity with frequency of the designed antenna is shown in Figure 13. It shows directivity of 7.54 dBi at lower resonance frequency (6 GHz) and 6.34 dBi at higher resonance frequency (7 GHz).

5. CONCLUSION

In this paper, an application of ANN is successfully implemented for the prediction of accurate slot size over a desired level of performance parameters. This ANN approach is simple and fast synthesis modeling scheme which produces more accurate results for slot size of the patch antenna with less computational time and least errors. For validation study of ANN output, an X-shaped RMSA is fabricated and measured results are found in good agreement with the IE3D and ANN results. This fabricated X-shaped RMSA is operating in dual frequency range at 6 GHz and 7 GHz and can be used for C-band applications such as in satellite communication.

ACKNOWLEDGMENT

The author is very grateful to Maulana Azad National Fellowship, University Grant Commission, New Delhi for providing financial assistance through senior research fellowship. We are also thankful to Prof. Ananjan Basu, Center for Applied Research in Electronics, IIT-Delhi, India for providing antenna measurement facility in his lab.

REFERENCES

1. Bahal, I. J. and P. Bhartia, *Microstrip Antennas*, Artech House, Boston, MA, 1985.
2. Nakano, H. and K. Vichien, "Dual-frequency square patch antenna with rectangular notch," *Electron. Lett.*, Vol. 25, No. 16, 1067–1068, 1989.
3. Lau, K. L., K. C. Kong, and K. M. Luk, "Dual-band stacked folded patch antenna," *Electron. Lett.*, Vol. 43, No. 15, 789–790, 2007.
4. Singh, A., J. A. Ansari, K. Kamakshi, A. Mishra, and M. Aneesh, "Compact notch loaded half disk patch antenna for dualband operation," *Ann. Telecommun.*, 2013, Doi: 10.1007/s12243-013-0383-6.
5. Vegni, L. and A. Toscano, "Analysis of microstrip antennas using neural networks," *IEEE Trans. Magn.*, Vol. 33, No. 2, 1414–1419, Mar. 1997.
6. Mishra, R. K. and A. Patnaik, "Neural network-based CAD model for the design of square-patch antennas," *IEEE Transactions on Antennas and Propagation*, Vol. 46, No. 12, 1890–1891, Dec. 1998.
7. Patnaik, A. R., K. Mishra, G. K. Patra, and S. K. Dash, "An artificial neural network model for effective dielectric constant of microstrip line," *IEEE Transactions on Antennas and Propagation*, Vol. 45, No. 11, 1697, Nov. 1997.
8. Mishra, R. K. and A. Patnaik, "Designing rectangular patch antenna using the neurospectral method," *IEEE Transactions on Antennas and Propagation*, Vol. 51, No. 8, 1914–1921, Aug. 2003.
9. Watson, P. M., K. C. Gupta, and R. L. Mahajan, "Development of knowledge based artificial neural network models for microwave components," *Proc. IEEE MTT-S Int. Microw. Symp. Dig.*, Vol. 1, 9–12, 1998.
10. Karaboga, D., K. Guney, S. Sagiroglu, and M. Erler, "Neural computation of resonance frequency of electrically thin and thick rectangular microstrip antennas," *Inst. Elect. Eng. Proc., Microw., Antennas Propag.*, Vol. 146, No. 2, 155–159, Apr. 1999.

11. Sagiroglu, S., K. Guney, and M. Erler, "Resonant frequency calculation for circular microstrip antennas using artificial neural networks," *Int. J. RF, Microw. CAE*, Vol. 8, 270–277, 1998.
12. Sagiroglu, S. and K. Guney, "Calculation of resonant frequency for an equilateral triangular microstrip antenna with the use of artificial neural networks," *Microw. Opt. Technol. Lett.*, Vol. 14, No. 2, 89–93, 1997.
13. Gopalakrishnan, R. and N. Gunasekaran, "Design of equilateral triangular microstrip antennas using artificial neural networks," *Proc. IEEE IWAT*, 246–249, 2005.
14. Guney, K., S. Sagiroglu, and M. Erler, "Generalized neural method to determine resonant frequencies of various microstrip antennas," *Int. J. RF, Microw. CAE*, Vol. 12, 131–139, 2002.
15. Guney, K. and N. Sarikaya, "A hybrid method based on combining artificial neural network and fuzzy inference system for simultaneous computation of resonant frequencies of rectangular, circular, and triangular microstrip antennas," *IEEE Transactions on Antennas and Propagation*, Vol. 55, No. 3, 659–668, Mar. 2007.
16. Guney, K. and N. Sarikaya, "Concurrent neuro-fuzzy systems for resonant frequency computation of rectangular, circular, and triangular microstrip antennas," *Progress In Electromagnetics Research*, Vol. 84, 253–277, 2008.
17. Turker, N., F. Gunes, and T. Yildirim, "Artificial neural design of microstrip antennas," *Turk. J. Elec. Eng.*, Vol. 14, 445–453, 2006.
18. Neog, D. K., S. S. Pattnaik, D. C. Panda, S. Devi, B. Khuntia, and M. Dutta, "Design of a wideband microstrip antenna and the use of artificial neural networks in parameter calculation," *IEEE Antennas Propag. Mag.*, Vol. 47, No. 3, 60–65, Jun. 2005.
19. Thakare, V. V. and P. K. Singhal, "Bandwidth analysis by introducing slots in microstrip antenna design using ANN," *Progress In Electromagnetics Research M*, Vol. 9, 107–122, 2009.
20. Thakare, V. V. and P. Singhal, "Microstrip antenna design using artificial neural networks," *Int. J. RF, Microw. CAE*, Vol. 20, 76–86, 2010.
21. Robustillo, P., J. Zapata, J. A. Encinar, and M. Arrebola, "Design of a contoured-beam reflectarray for a EuTELSAT European coverage using a stacked-patch element characterized by an artificial neural network," *IEEE Antennas Wireless Propag. Lett.*, Vol. 11, 977–980, 2012.
22. Wang, Z., S. Fang, Q. Wang, and H. Liu, "An ANN-based synthesis model for the single-feed circularly-polarized square microstrip antenna with truncated corners," *IEEE Transactions on Antennas and Propagation*, Vol. 60, No. 12, 5989–5992, Dec. 2012.
23. Freni, A., M. Mussetta, and P. Pirinoli, "Neural network characterization of reflectarray antennas," *Int. J. Antennas Propag.*, Vol. 2012, 541354-1–541354-10, 2012.
24. Akdagli, A., A. Toktas, A. Kayabasi, and I. Develi, "An application of artificial neural network to compute the resonant frequency of E-shaped compact microstrip patch antennas," *Journal of Electrical Engineering*, Vol. 64, No. 5, 317–322, 2013.
25. Khan, T. and A. Dey, "Prediction of slot size and inserted air gap for improving the performance of rectangular microstrip patch antennas using artificial neural networks," *IEEE Antennas Wireless Propag. Lett.*, Vol. 12, 1367–1371, Oct. 2013.
26. IE3D. Ver. 14.0, Zeland Software, Inc., Fremont, CA, USA, Oct. 2007.
27. Higham, D. J. and N. J. Higham, "MATLAB guide," *SIAM*, Philadelphia, PA, USA, 2005.
28. Sivia, J. S., A. P. S. Pharwaha, and T. S. Kamal, "Analysis and design of circular fractal antenna using artificial neural networks," *Progress In Electromagnetics Research B*, Vol. 56, 251–267, 2013.
29. Hagan, M. T. and M. B. Menhaj, "Training feedforward networks with the Marquardt algorithm," *IEEE Trans. Neural Netw.*, Vol. 5, No. 6, 989–993, Nov. 1994.